J. Fluid Mech. (1991), *vol.* 232, *pp.* 47–72
Printed in Great Britain

Low-frequency pressure oscillations in a model ramjet combustor

By KEN H. YU[1]†, ARNAUD TROUVÉ[2] AND JOHN W. DAILY[3]

[1] Department of Mechanical Engineering, University of California, Berkeley, CA 94720, USA

[2] Center for Turbulence Research, Stanford University, Stanford, CA 94305, USA

[3] Department of Mechanical Engineering, University of Colorado, Boulder, CO 80309, USA

(Received 1 March 1990 and in revised form 14 March 1991)

Low-frequency combustion instabilities are studied in a model ramjet combustor facility. The facility is two-dimensional, and is comprised of a long inlet duct, a dump combustor cavity with variable size capability, and an exhaust nozzle. The flame is observed to be unstable over a wide range of operating conditions. Acoustic pressure and velocity measurements are made at various locations in the system. They show that the inlet duct acts as a long-wavelength acoustic resonator. However, the instability frequency does not lock to any particular value. This result suggests that the instability mechanism is not purely acoustic in nature. Schlieren imaging reveals that the instability is associated with large-scale flame-front motions which are driven by periodic vortex shedding at the instability frequency. Vortices are generated at the dump in phase with the acoustic velocity fluctuations in the inlet duct. The unsteady heat addition process closely follows the vortex history: the vortices form, grow in size, convect through the combustor cavity, impinge on the exhaust nozzle, break down to small scales and burn. C_2 and CH radical spectroscopy is used to determine the phase relation between heat release and pressure in the reaction zone. Rayleigh's criterion is thereby shown to be satisfied. Next, the crucial question of how the oscillation frequency is determined is addressed. Inlet velocity and combustor length are systematically varied to assess the role of vortices by modification of their characteristic lifetime. The influence of the acoustic feedback time is also studied by shortening the inlet duct. The results show that the instability frequency is controlled by both vortex kinetics in the combustor and acoustic response of the inlet section. Therefore, the instability may be considered as a mixed acoustic–convective mode. Finally, combining Rayleigh's criterion with a global feedback loop equation, it is found that the resonant frequencies are selected according to the restriction

$$\frac{1}{4N-1} < \frac{\tau_v}{\tau_f} < \frac{3}{4N-3},$$

where N is the mode of oscillation and τ_v is the time for vortices to be convected from inlet to exhaust with τ_f being the feedback time taken for a pressure disturbance to travel up the inlet system and back.

1. Introduction

Ducted systems featuring a source of heat are susceptible to spontaneous oscillations. Ramjets and afterburners, as well as many power devices, exhibit

† Present address: Research Department, Naval Weapons Center, China Lake, CA 93555, USA.

undesirable combustion instabilities under certain operating conditions, at levels that eventually cause loss of performance and damage. Growing pressure oscillations and large flame-front motions generally reach a quasi-periodic limit cycle. They may also lead to extinction due to flashback or flame blow-off.

Our work has been motivated by a desire to understand the nature of the coupling process which leads to large-amplitude, low-frequency pressure and combustion oscillations in ramjet combustors. Although there has been extensive study of the problem, it remains interesting because of the complexity that arises out of the large number of coupling interactions that are possible. The complexity comes from the nature of the flow field in the flame region which contains turbulent jets, recirculation zones, mixing layers, flow through a nozzle, etc.

In the past, most of the experimental work has focused on dump combustors with open outlets. However, ramjet combustors feature closed geometries with an exhaust nozzle. In this configuration, coupling interactions are possible either between the flame zone and the acoustic field (acoustic modes), or between flow instabilities in the reaction zone and the exhaust nozzle (convective modes).

1.1. *Acoustic modes*

Early studies of singing flames (Putman 1971) have shed light on the crucial role of the natural vibrational modes of sound waves in the combustion system. In many situations, the coupling between acoustics and the combustion processes is responsible for sustaining the instability. This destabilizing mechanism was first identified by Rayleigh (1878, 1945): oscillations are amplified when pressure and heat release fluctuations are positively correlated in time (see also Chu 1956). Recent experimental investigations (Smith & Zukoski 1985; Poinsot *et al.* 1987; Sterling & Zukoski 1987; Hedge *et al.* 1987; Langhorne 1988) support the description of low-frequency instabilities in dump combustors as a result of similar interactions between the flame zone and the longitudinal acoustic modes of the whole system. It is therefore common practice to analyze these instabilities using phase arguments with respect to pressure and energy release.

Experimental visualizations also indicate that vortex shedding is a dominant factor in the instability mechanism. When the magnitude of the velocity fluctuation at the combustor inlet is high relative to the mean flow speed, the flow surges periodically into the chamber and large vortices are formed at the instability frequency (Smith & Zukoski 1985; Poinsot *et al.* 1987). Early evidence of the role of vortical structures during unstable operation is attributed to Rogers & Marble (1956). In their study of high-frequency or 'screech' instabilities, they propose a general mechanism which described the energy exchange between the oscillating pressure field and the flame zone: transverse acoustic perturbations force periodic vortex shedding at the dump; these vortices then transport combustible material into the hot wake of the flame stabilizer and burn after a certain delay time; the resulting pressure pulses, when appropriately phased, feed energy back to the acoustic field and the loop is closed in a resonant manner. Since the combustion of the vortices provides the perturbations in energy release, the instability is said to be vortex driven.

Several conditions must be satisfied to sustain the instability.

(i) The instability scenario relies on large acoustic velocity fluctuations at flow separation and consequent vortex formation. High acoustic gains are therefore needed and unstable frequencies are most likely found close to the acoustic eigenfrequencies of the combustion system (Crump *et al.* 1986; Poinsot *et al.* 1987),

(ii) The heat release from the combustion of the vortices needs to occur with appropriate phasing with respect to pressure oscillations. This condition is expressed by Rayleigh's criterion,

(iii) Furthermore, the instability mechanism features a characteristic delay time between vortex shedding and burning. If the heat release were spatially and temporally distributed, not much return would be expected to the acoustic field. General observations, however, indicate that most of the energy release is locally concentrated and happens during a short interval within the instability cycle. This pulsatile nature of combustion oscillations is probably associated with vortex breakdown and intense turbulence–combustion interactions.

For instance, by correlating schlieren images with phase-averaged flame radiation distributions, Poinsot *et al.* (1987) were able to trace out the combustion history in shed vortices during an intense low-frequency instability mode. It is seen that multiple flame interaction produces small-scale vortex breakdown, vigorous mixing, and rapid and intense reaction. With suitable timing with respect to pressure, these peaks in heat release are capable of sustaining large-amplitude oscillations. Similar pulsating combustion phenomena are reported by Smith & Zukoski (1985) in a rearward-facing-step experiment. Vortex breakdown is then caused by impingement on a lateral wall of the combustor.

1.2. *Convective modes*

It is often suggested that flames in enclosures may exhibit original unstable behaviour. Common arguments lay emphasis on dynamic aspects related to impingement of shear layers on the exit nozzle. Isothermal flow studies indicate that such situations may develop vortex-driven coherent oscillations (Rockwell 1983). For instance, Ho & Nosseir (1981) describe purely hydrodynamic oscillations produced by a free jet impinging on a flat plate. This situation arises at high subsonic Mach numbers and is based on a resonant interaction between a shear flow and a solid boundary. The mechanism may be explained as follows: Kelvin–Helmholtz vorticity waves develop in the jet mixing layers and lead to vortex formation, these vortices are then convected downstream, interact with the obstacle, and reflect pressure perturbations, which in turn modulate the shedding process. In ducted systems, this vorticity mode eventually couples with acoustics; but the oscillations need not occur at the sound wave eigenfrequencies (Jou & Menon 1987). So far, the relevance of this instability mechanism to combustion problems remains an open issue.

Exhaust nozzle dynamics also need to be considered. Convected temperature perturbations may be viewed as incident entropy waves. When passing through the nozzle, a modulation of the mass flow rate is induced and consequently pressure waves are generated. As shown by Marble & Candel (1977), the reflected pressure wave amplitude increases with the combustor Mach number. At fixed incident flow conditions, maximum feedback is obtained when the nozzle is choked. With appropriate phasing, and sufficiently high velocities, coupled entropy–acoustic modes may be excited (Abouseif, Keklak & Toong 1984; Humphrey & Culick 1987).

While purely acoustic modes have received considerable attention in the past decade, theoretical speculations suggest that convective waves are likely to be a major factor in closed chamber instabilities. Lack of experimental evidence motivates the present study. In the following, we study low-frequency instabilities in a combustion chamber cavity with a sudden expansion at the inlet and downstream contraction at the outlet. The configuration simulates a ramjet engine situation

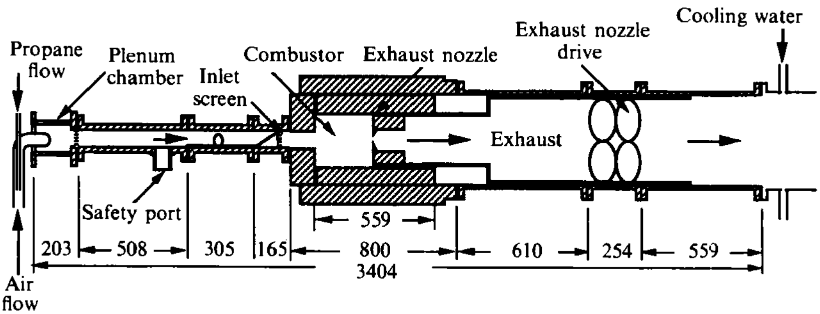

FIGURE 1. Two-dimensional combustion tunnel facility with variable-geometry test section. (Dimensions in mm.)

where the flow is accelerated to sonic conditions at the exhaust nozzle. However, in the present series of experiments, the flow is everywhere subsonic in the combustor and the outlet is not choked. The facility and diagnostic techniques are described in §2. The flame is observed to be unstable over a wide range of operating conditions. The instability is dominated by periodic vortex shedding of large vortices that impinge on the exhaust nozzle. Oscillating combustion is coupled with acoustic fluctuations in the inlet duct. A detailed analysis of the instability mechanism is presented in §3.1. Systematic variations of the inlet fluid velocity and combustor and inlet geometry are described in §3.2. They induce significant frequency shifts which demonstrate that the instability should be understood as a coupled acoustic–convective mode (§4).

2. Experimental system and instrumentation

2.1. *Combustion tunnel*

The two-dimensional variable-geometry combustion tunnel used in the experiments is shown in figure 1. Two compressors provide air to the facility up to a maximum flow rate of 0.5 kg/s. A desiccant dryer and a Balstor air filter are used to dry and filter the air. Propane is added to the air by opposed flow injection. The opposed flow injection is used to promote thorough premixing before the mixture enters the inlet section. The fuel and air lines are metered by sonic nozzles. Pressure transducers (Senso-Metric model SP91) sense the pressure upstream of each nozzle with an accuracy of 1 % of full scale.

The inlet section is comprised of a plenum chamber and an inlet duct. The plenum chamber is 20.3 cm long. The duct is configured for two different lengths, 113.2 cm long and 31.9 cm long. It is 2.5 cm high and 17.6 cm wide. Eight instrumentation ports allow pressure and velocity measurements at various locations in the duct. It is also equipped with a brass foil safety port which has been designed to blowout at excessive pressure. Inside the inlet duct, two square-mesh wire screens are mounted normal to the incoming flow. The screens are 16 mesh/in. stainless steel with 0.24 mm wire diameter. They are used to flatten the inlet velocity profile, reduce the turbulence level, and to provide flashback protection. The location of the second screen can be adjusted between 0 and 26.5 cm upstream from the dump plane.

The double-step combustor is shown in figure 2. The steps are 2.5 cm high. The exit nozzle features a sudden contraction with a 0.5 cm × 17.6 cm orifice. The test section is designed for variable geometry. The length of the combustion chamber is adjusted by changing the location of the exhaust nozzle with a gear and rack assembly. The

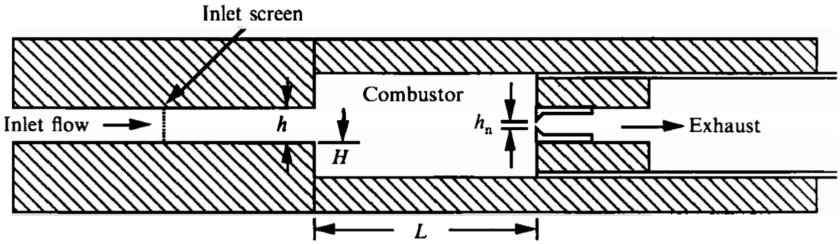

FIGURE 2. Combustor test section showing the design parameters: width = 173 mm; $H = 25$ mm; $h = 25$ mm; $h_n = 5$ mm; L varies from 50 to 500 mm.

length is varied from 5.8 cm to 15 cm. Optical access to the reaction zone is provided by lateral quartz windows. These windows are approximately 2.5 cm thick and give full access to the test section, thereby allowing direct examination of the flame structure, schlieren imaging and chemiluminescence measurements.

2.2. *Acoustic measurements*

Wall pressure measurements are performed using Kistler model 206 piezoelectric transducers along with a Kistler model 5126 Piezotron coupler. Pressure transducers can be mounted along the inlet duct, combustion chamber, and exhaust section. Water-cooled adapters are used during combustion.

The velocity in the inlet duct is measured using a hot-film probe. The equipment includes a TSI model 1054A constant-temperature anemometer system and a TSI 1210-20 cylindrical element probe.

Signals are first amplified and filtered. Then, they are sampled with a Zenith Data Systems personal computer, equipped with a MetraByte Dash-16 A/D board which allows simultaneous sampling of up to 8 differential analog signals. Typically, 4096 data points are taken at a sampling frequency of 1000 Hz. Spectral analysis of the signals is performed using the fast Fourier transform technique.

2.3. *Phase-sensitive visualization*

The unstable flames are visualized by a phase-sensitive schlieren imaging technique that uses a conventional television camera (Trouvé, Yu & Daily 1987). Since the standard video rate of 30 Hz is slower than the instability frequencies, a stroboscopic technique must be used. The basis of the method lies in coupling a short-pulsed light source with the vidicon tube video camera. When a quasi-periodic unstable mode is excited in the combustion system, the signal delivered by a pressure transducer mounted on the combustor may be used as a reference signal. After filtering and amplification, this signal is sent to a pulse generator with variable-phase capability. The delayed output of the pulse generator is in turn used to trigger the flashlamp. By varying the phase of the generator signal, one can effectively trace out an entire period of a repeatable process. The images acquired by the camera can be conveniently recorded on a video tape for later playback or digitized directly into computer memory. The images can then be analysed using a computer-based image processing system.

The schlieren system features a typical Z configuration. An EG&G Electro-Optics model FX-800 flashtube coupled with an EG&G model FY-903 trigger module provides a spark light source. The light from the spark source is collimated by a 3.94 m focal length, 0.3 m diameter spherical mirror. The collimated light passes through the test section and is refocused by another identical mirror onto a schlieren stop. The light through the schlieren stop is then imaged onto a camera detector surface by an imaging lens.

2.4. *C_2 and CH emission measurements*

To improve our understanding of the instability driving mechanism it is necessary to collect some information on the heat release processes. A simple technique that traces the rate of combustion consists in measuring the radiation intensity of free radicals such as C_2 or CH. These radicals appear almost exclusively in the reaction zones, and their emitted light intensity can be directly related to the chemical reaction rate or, equivalently, to the heat release rate. The relation may be assumed linear (Poinsot *et al.* 1987; Langhorne 1988).

The light emitted by the flame is imaged by a convex lens onto a RCA IP28 photomultiplier. The entire combustor region or a sub-region may be imaged. A narrowband interferential filter is mounted on the photomultiplier and isolates characteristic C_2 or CH emission bands. The filter bandwidth is 5 nm. The selected wavelengths for C_2 and CH are 516 nm and 431 nm respectively.

3. Experimental results

The control parameters in operating the model combustor are the inlet jet reference velocity, the equivalence ratio, the combustor geometry, and the inlet duct geometry. The combustor has been operated over a range of reference velocities from 10 to 30 m/s, and equivalence ratios from the lean mixture flammability limit to near stoichiometry. The lean limit behaviour is similar to other combustors as shown in figure 3.

At low equivalence ratios, close to the lean flammability limit, it is possible to operate the combustor in a stable mode. At higher equivalence ratios, typically around 0.6 and above, the combustion process becomes highly unstable, exhibiting large-amplitude pressure oscillations. Figure 4 shows several pressure records under some typical unstable operations. The records display a low-frequency oscillatory behaviour with significant cycle-to-cycle variations. The corresponding power spectra (figure 5) are characterized by either a single peak or a peak and its higher harmonics.

A detailed study of one unstable case (§3.1) shows some features that are characteristic of an acoustic mode while other experiments, in which the control parameters are systematically varied (§3.2) show contrary evidence. Most interestingly, the instability frequency does not lock to any particular value. This result suggests that the instability mechanism is not purely acoustic in nature. Both sets of experiments are presented below.

3.1. *Detailed observation of a single case*

To improve our understanding of the basic physical mechanisms involved, one case is investigated in detail. The reference velocity for the case is 14.4 m/s and the equivalence ratio is 0.58. The inlet duct length and combustor length are fixed at 1.13 m and 0.100 m, respectively. The combustor pressure oscillation under this particular operating condition does not have much cycle-to-cycle variation, and hence the signals are highly repeatable. This provides a favourable condition to apply our phase-sensitive schlieren imaging technique. The main resonant frequency occurs at about 65 Hz for this case.

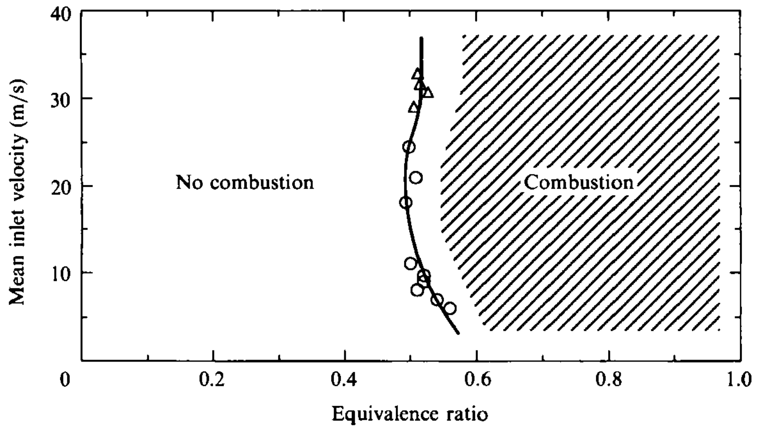

FIGURE 3. Lean mixture flammability limit for the combustor. ○, Combustor length = 100 mm; △, 150 mm.

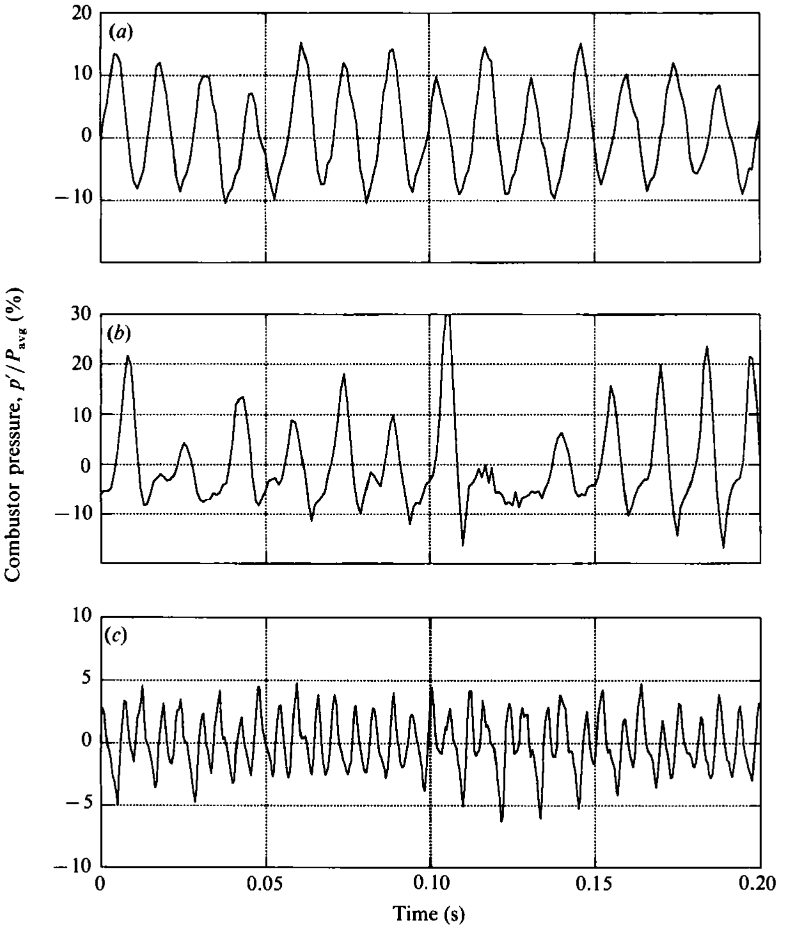

FIGURE 4. Combustor pressure records during typical unstable mode operations. The operating conditions are the following: (*a*) $U_{ref} = 18.5$ m/s, $L = 0.100$ m, and $\phi = 0.65$; (*b*) $U_{ref} = 14.4$ m/s, $L = 0.150$ m, and $\phi = 0.65$; (*c*) $U_{ref} = 18.5$ m/s, $L = 0.075$ m, and $\phi = 0.60$.

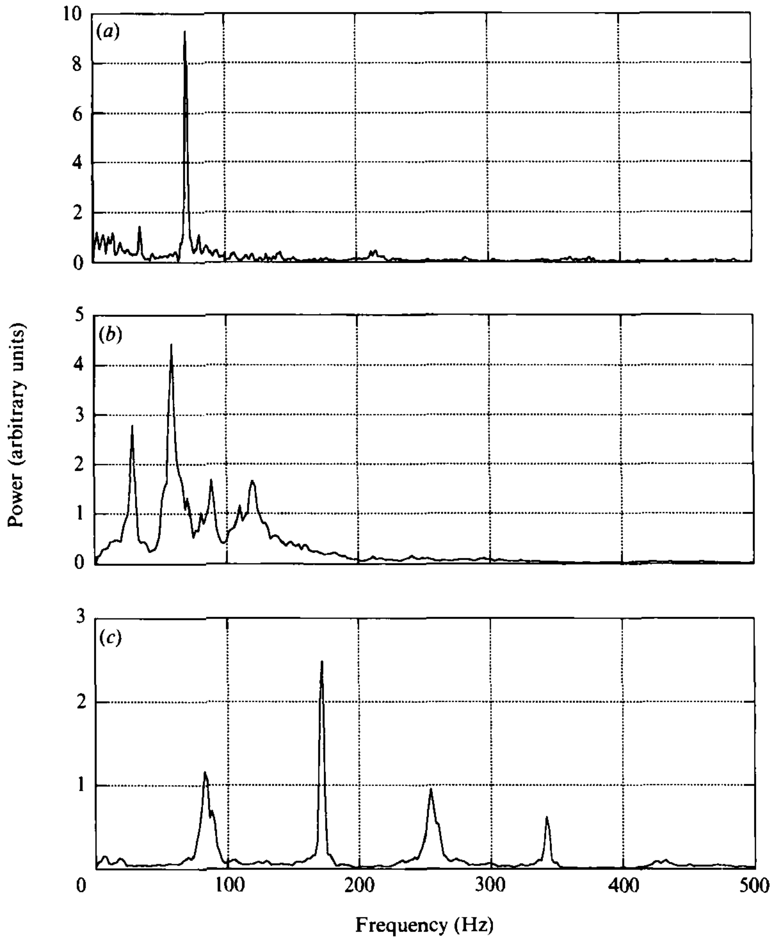

FIGURE 5. Power spectra corresponding to figure 4.

3.1.1. *Organized pressure and velocity variations*

Since acoustically coupled instabilities have been observed in many combustor configurations, the characterization of the acoustic response of the facility is now a standard experimental procedure. In the present study, the modal structure of the pressure field during unstable conditions is investigated directly by performing extensive pressure measurements along the entire facility. Results are shown in figure 6. The raw data are used to calculate the axial distribution of the normalized spatial cross-correlation coefficient of the local pressure with respect to pressure in the combustor. The measurements show that the pressure field in the inlet duct exhibits a well-organized structure. On the other hand, the oscillations in the exhaust pipe downstream of the combustor cavity are shown to be uncorrelated to the upstream pressure, which suggests that the combustor exit nozzle acts as a downstream acoustic boundary for the frequency of interest.

Figure 7 shows the amplitude of the 65 Hz peak as a function of streamwise location in the inlet duct. Data are normalized by the fluctuating pressure amplitude inside the combustor, which is about 1 psig (over 170 dB). The amplitude variations exhibit a characteristic standing half-wave pattern. Furthermore, the flame zone is located near a pressure antinode and, as suggested by Rayleigh's (1878, 1945)

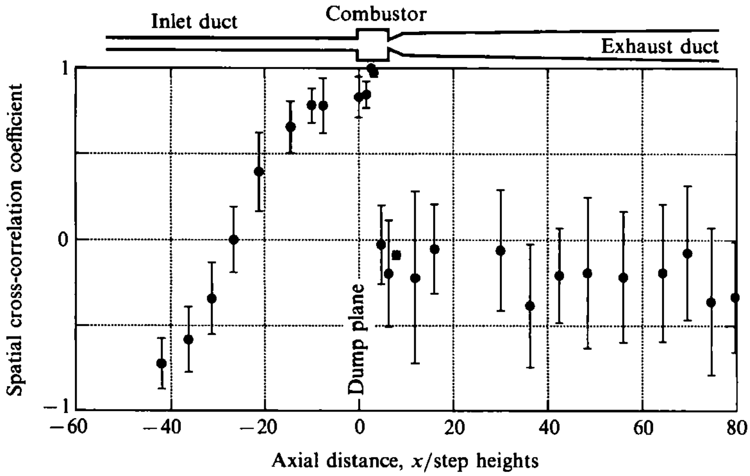

FIGURE 6. Spatial cross-correlation coefficient of local pressure at x with respect to the combustor pressure at x_0. The coefficient is defined as:

$$C(x) = \int_0^T P(x_0,t)\,P(x,t)\,\mathrm{d}t \bigg/ \left(\int_0^T P^2(x_0,t)\,\mathrm{d}t \int_0^T P^2(x,t)\,\mathrm{d}t\right)^{\frac{1}{2}},$$

where P is the measured acoustic pressure and T is the instability period.

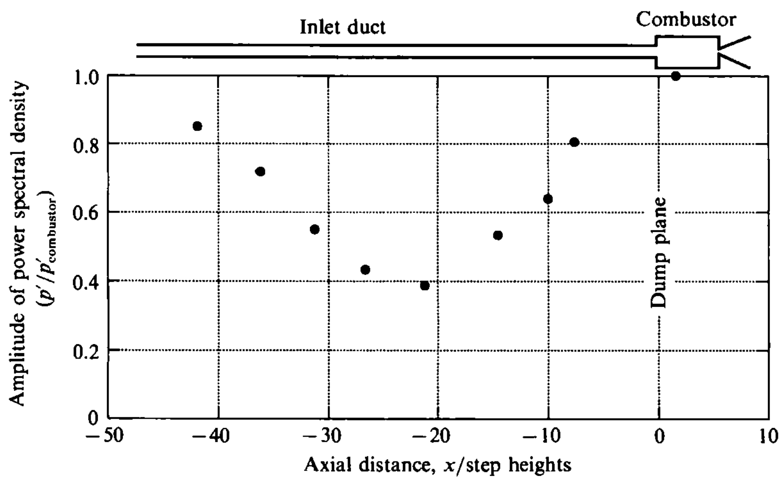

FIGURE 7. Amplitude distribution of the pressure spectral density at the instability frequency along the inlet duct wall.

criterion, this situation is favourable for developing coupled acoustic–combustion modes.

The centreline velocity throughout the inlet region is measured using the hot-film probe. The flow is oscillated at the instability frequency and exhibits intense fluctuations of the order of the mean velocity. Figure 8(*a*) shows a typical velocity record, measured 19 cm upstream of the combustor dump. Its phase difference with the combustor pressure is also shown. Since the acoustic wavelength is greater than 5 m, these records provide a fair estimation of the phase difference between velocity and pressure at the dump. It shows that the inlet velocity leads the combustor pressure by approximately $\frac{1}{4}$ of the instability period.

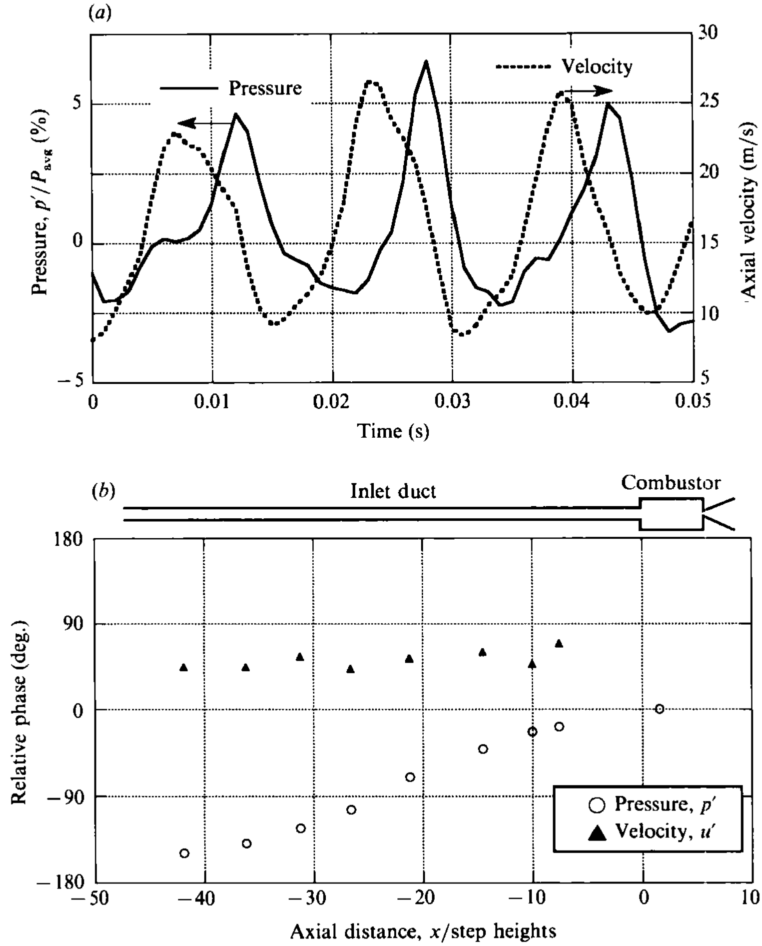

FIGURE 8. Measurements of inlet velocity and acoustic pressure with respect to the combustor pressure. (a) Simultaneous measurements of inlet velocity and combustor pressure. (b) Relative phases of acoustic pressure and velocity along the inlet duct. The combustor pressure phase is used as the reference phase.

Figure 8(b) shows the phase distribution for both velocity and pressure with respect to combustor pressure. Centreline velocities have a nearly constant phase, independent of the axial distance. Similar results are found in the case of an oscillating flow through a pipe driven by a periodic pressure difference (Schlichting 1979). The phase of wall pressure, however, varies along the inlet duct. This implies that the velocity profile inside the inlet duct is a function not only of time but also of axial distance. The phase variation of wall pressure is consistent with the standing half-wave pattern shown in figure 7.

3.1.2. *Schlieren visualization*

Using the combustor pressure signal as a reference signal, we applied the phase-sensitive schlieren imaging technique and took several pictures of the flame zone throughout the instability cycle. Schlieren photographs trace out the interface between cold reactants entering the chamber and hot burnt products. They provide some visual understanding of the fluid dynamics in the combustor. In particular, they reveal the presence of large-scale vortices in the flow. These vortices form, grow

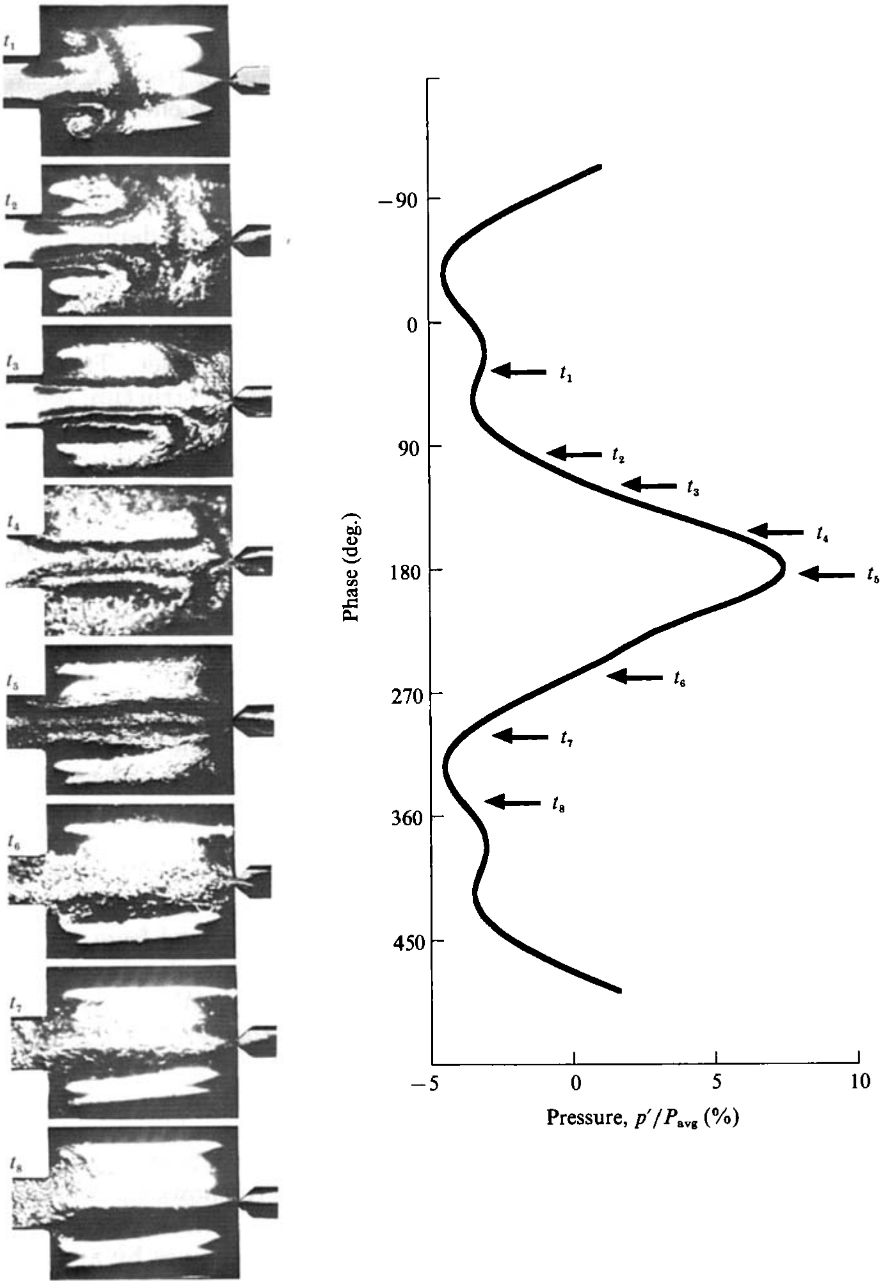

FIGURE 9. A sequence of phase-locked schlieren photographs of the combustor during an unstable mode operation. The trace shown is the pressure record of one instability cycle. The photographs are taken at the respective phases marked on the trace.

in size, impinge on the exhaust nozzle, break down and burn periodically at the instability frequency. A sequence of frames with corresponding phase location is displayed in figure 9.

At time t_1, the pressure in the combustor is very low while, as inferred from figure 8(*a*), the inlet flow acceleration is maximum. The flames stabilized behind the steps are seen to roll up into growing vortices. These vortices entrain a large amount of combustible material into the hot recirculation zones. The picture suggests that the flow is symmetric and essentially two-dimensional.

Vortices are then rapidly convected through the combustor (times t_2 and t_3). They grow into a large 'mushroom' structure that spreads over the entire chamber cross-section. The velocity is maximum close to time t_3.

Time t_4 is just prior to the impingement of the vortical structure on the exhaust nozzle. The combustor pressure is still rising and the inlet velocity is still above the mean level. However, as the inlet flow is being decelerated, the flames lift from the edges of the steps and start propagating upstream.

Time t_5 corresponds to maximum pressure in the cavity. With the impingement of the vortical structure on the exhaust nozzle, unburnt reactants are pushed out through the nozzle, thereby venting the combustion chamber. The combustor pressure then begins to drop sharply. Meanwhile the vortical structure breaks down at the exhaust nozzle. As indicated by figure 8(a), the fluid at inlet is strongly decelerated and as a consequence the flame fronts penetrate deeper into the incoming flow. Volume expansion due to heat release must also contribute to the velocity reversal.

Minimum velocity occurs between times t_6 and t_7. The incoming flow is slowed to a stop and even reversed. Owing to the shortage of reactants, partial extinction occurs in the combustion chamber. Time t_7 shows a combustor almost free of any chemical reaction. Direct views of the facility show some blue emission from the gas in the inlet duct where flashback is taking place.

At the next instant t_8, the pressure is close to minimum and the velocity is again rising with a steep acceleration. Fresh reactants surge inside the combustor, thereby producing a strong shear at flow separation, and new vortices are consequently shed. Reformation of a two-dimensional flame is then observed. An image of a later instant would exhibit the same vortical pattern as at time t_1.

An interesting aspect of the data is the coincidence of the arrival of the vortical structure at the nozzle with the peak of the pressure. When the structure impinges on the nozzle, the density ratio across the exit orifice is increased from the burnt gas to unburnt gas value. Thus the mass flow rate through the nozzle must correspondingly increase and the pressure drop sharply. We believe this is an important mechanistic event that determines, in part, the period of the instability.

3.1.3. *Heat addition processes*

C_2 and CH radical spectroscopy is used to describe the heat addition processes. The emitting area seen by the photomultiplier comprises the combustor cavity but does not include either the inlet duct or the nozzle. Figure 10 shows the phase relation between the time-resolved C_2 and CH emission intensity and the combustor pressure. It shows that the heat release rate trails the combustor pressure by approximately $\frac{1}{4}$ of a period.

By analysis of the schlieren and chemiluminescence data, it may be seen that the heat release rate closely follows the vortex history. When vortices are formed, the heat release rate is close to minimum. While the vortices are convected through the combustor, the contact area between cold reactants and hot products increases. This causes a higher rate of mixing between the fluids, and the heat release rate increases accordingly. The maximum heat release rate occurs shortly after the vortices impinge on the exhaust nozzle. It appears that the impingement breaks up the large vortical structure, enhances small-scale mixing, and thereby produces rapid burning of the fresh mixture that has been trapped within the structure.

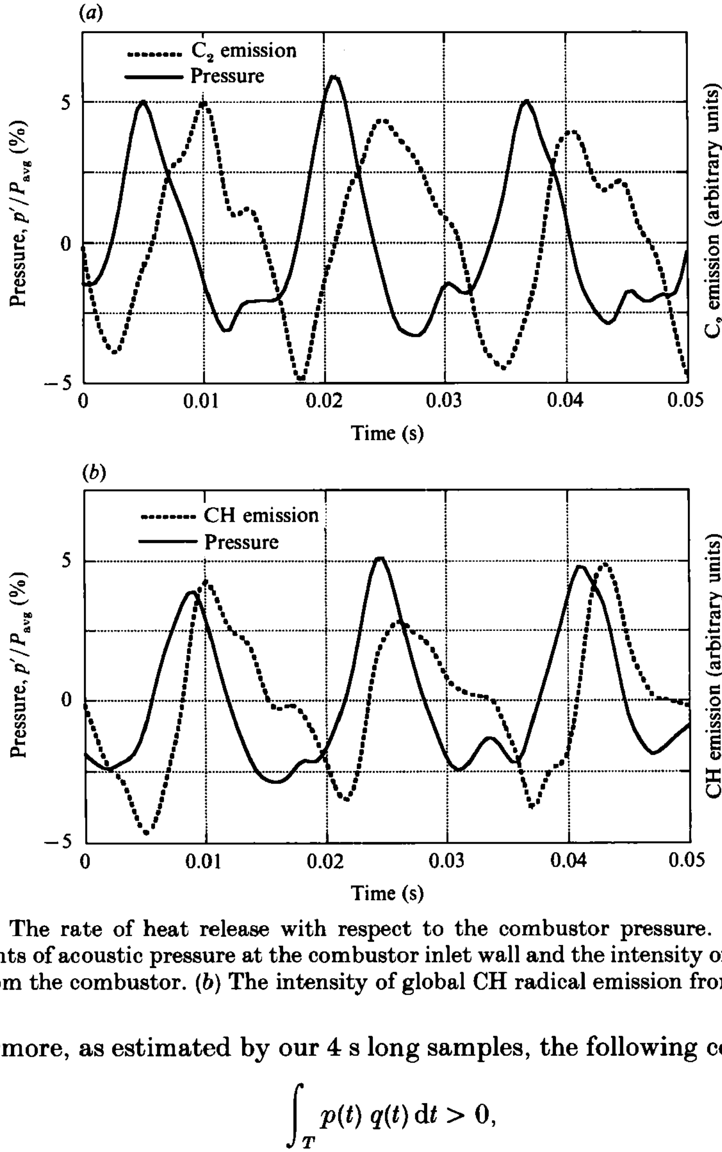

FIGURE 10. The rate of heat release with respect to the combustor pressure. (*a*) Simultaneous measurements of acoustic pressure at the combustor inlet wall and the intensity of global C_2 radical emission from the combustor. (*b*) The intensity of global CH radical emission from the combustor.

Furthermore, as estimated by our 4 s long samples, the following condition holds:

$$\int_T p(t)\, q(t)\, \mathrm{d}t > 0,$$

where $p(t)$ and $q(t)$ designate respectively unsteady pressure and global heat release in the combustor. T is the instability period. This condition is an expression of Rayleigh's driving criterion. As discussed by Poinsot *et al.* (1987), the correlation function above is a source term in the acoustic energy balance of the system. If positive, energy is added to the oscillations and amplification occurs. When a limit cycle is reached, amplitudes are roughly constant in time. The source term then vanishes, keeping a slightly positive value to balance inherent system losses.

3.2. *What determines the instability frequency?*

From the results of the previous section, it is clear that the system acoustics play an important role in determining the nature of the instability. The inlet duct acoustics drive a large-amplitude modulation of the incoming flow rate and control vortex

Combustor length (mm)	Inlet velocity (m/s)	Equivalence ratio	Observed instability frequency (Hz)
58	12.3	0.65	74.3
	14.3	0.65	78.2
	16.3	0.65	82.1
	18.5	0.65	176.0
	20.6	0.65	188.7
80	12.2	0.65	69.7
	12.2	0.65	69.7
	14.2	0.65	71.4
	16.3	0.65	75.3
	18.2	0.66	77.2
	20.4	0.65	135.9
103	12.3	0.66	56.7
101	14.3	0.65	63.5
101	16.2	0.65	69.4
101	18.3	0.66	70.4
101	20.3	0.65	72.3
125	12.3	0.65	49.9
	14.4	0.65	54.7
	16.5	0.65	64.5
	18.5	0.65	69.4
150	12.3	0.65	57.7
	13.3	0.66	60.6

TABLE 1. Instability frequencies observed during various operating conditions. (Long inlet configuration.)

formation. The rate of heat release is determined by the dynamics of the vortex roll-up and break-up process. According to Rayleigh's criterion, suitable timing of heat addition with respect to pressure sustains the acoustic oscillations and allows periodic repetition of the unstable behaviour. However, the results are not sufficient to decide whether the instability frequency is determined directly by resonance in the inlet acoustics, by residence time considerations of fluid elements within the combustor, or by a combination of both.

In the following, the control parameters are systematically varied (§§3.2.1 and 3.2.3) and the system acoustics are analysed (§3.2.2) in an effort to clarify the basic physical mechanisms which determine the instability frequency. The results demonstrate the dual nature of the instability mode. In particular, the oscillation frequency is governed by both acoustic wave propagation in the inlet duct and vortex convection within the combustor.

3.2.1. *Parametric variation of velocity and combustor length*

When the flow features inside the combustor cavity are modified by systematic variations of injection speed and combustor length, the schlieren records show that the pulsatile nature of the instability is unaffected. The results of spectral analysis of pressure records are summarized in table 1 and shown in figure 11. In general, the instability frequency is a smooth and continuously increasing function of the flow rate (mode I). However, quite different behaviour is also observed at certain operating conditions. A small increase in the inlet velocity leads to a sudden hopping of the instability frequency to its first harmonic (mode II). Such abrupt changes in the instability frequency are characteristic of a resonant system response.

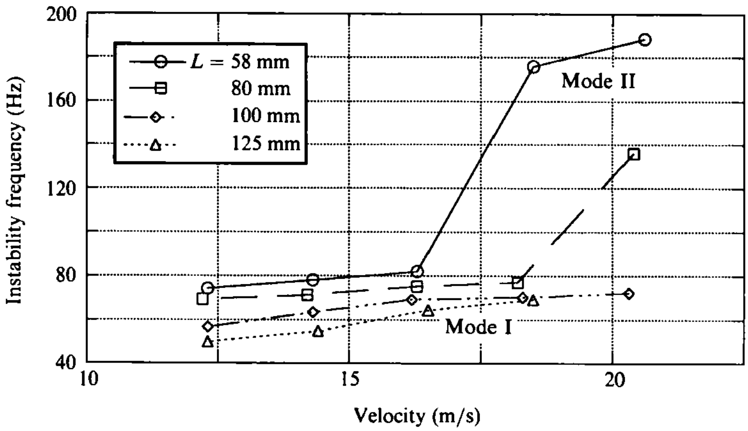

FIGURE 11. Measured frequency of oscillation as a function of inlet velocity and combustor length, L. The equivalence ratio ϕ is fixed at 0.65.

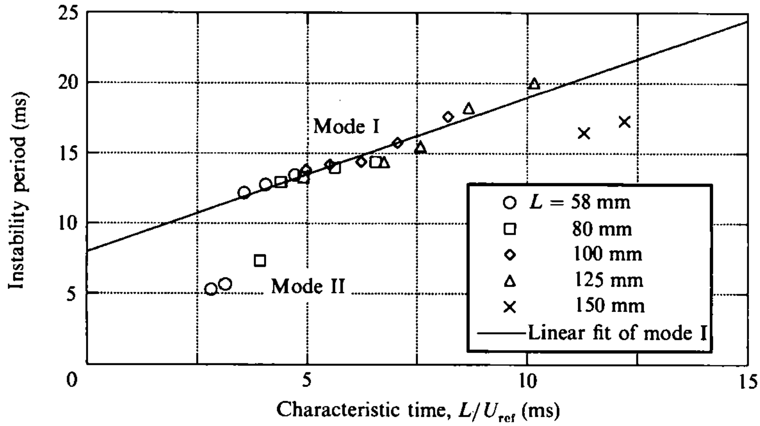

FIGURE 12. Measured period of oscillation as a function of the characteristic flow residence time L/U_{ref}.

Now defining a flow characteristic time as the combustor length L divided by the average inlet bulk velocity U_{ref}, the instability period is plotted as a function of this convection time in figure 12. The data points corresponding to mode I fall on a straight line which, according to a linear regression, has a slope of 1.1 and an intercept of 8 ms. The intercept time of 8 ms coincides with the round-trip time of a pressure wave travelling up the inlet system and back. Thus, it appears that the instability mechanism is controlled by two important timescales – a convection time and an acoustic time. The instability period is simply the sum of the two timescales, or an integral fraction of the sum.

Interestingly, a vortex lifetime, which includes vortex formation at the dump, convection through the cavity, impingement on the exhaust nozzle, breakdown to small scales and chemical reaction, is well estimated by L/U_{ref}. This allows the instability period to be expressed in terms of the vortex lifetime:

$$T_i = \frac{\tau_v + \tau_f}{N}, \tag{1}$$

where T_i is the instability period, τ_v is the vortex lifetime, τ_f is the acoustic

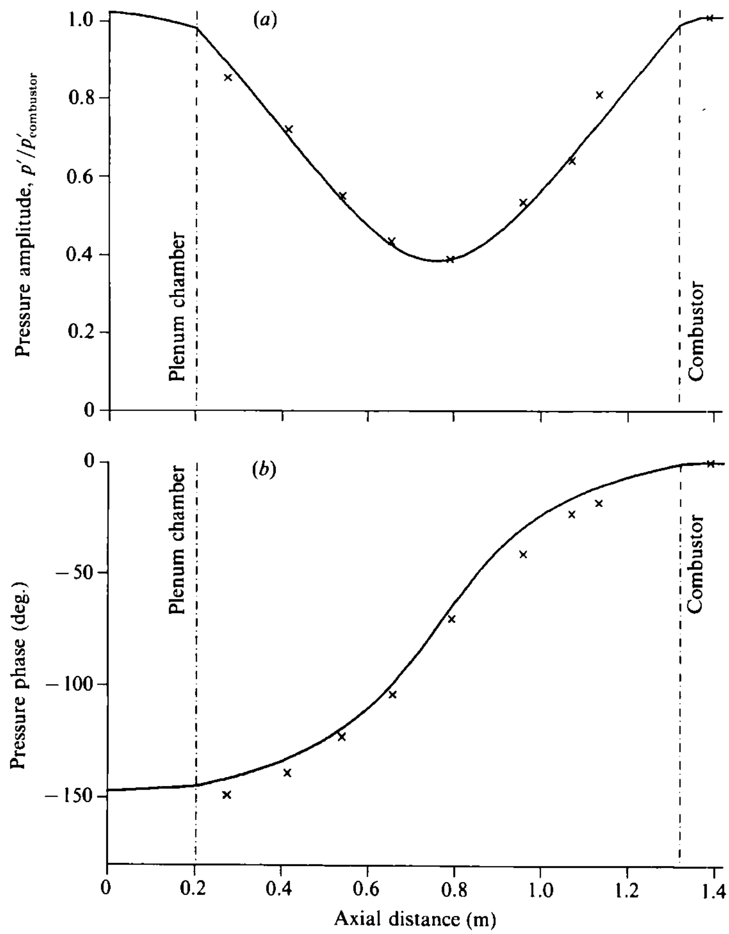

FIGURE 13. Computed acoustic response of the ducted system. The system is forced by an harmonic volume source which is located in the combustor and driven at the instability frequency of 65 Hz. —, calculation; ×, measured. (*a*) Acoustic pressure amplitude distribution in the inlet duct. (*b*) Acoustic pressure phase distribution in the inlet duct.

characteristic time for the inlet duct to respond, and N is a positive integer representing the mode number.

3.2.2. *Analysis of the acoustic resonator*

To better understand the system acoustics, a linear analysis of the longitudinal sound wave modes is performed. The analysis uses plane wave acoustic theory and a one-dimensional lumped parameter model (Crump *et al.* 1986; Poinsot *et al.* 1987). Since the acoustic wavelengths under consideration are much longer than the combustor length, the analysis is greatly simplified by treating the flame zone as a compact acoustic source. In this situation, the effect of heat addition on the acoustic field may be modelled as an harmonic volume source located inside the combustor.

The calculation takes into account the actual geometry of the inlet duct including the presence of a plenum chamber at the upstream end. The upstream boundary condition is estimated using the pressure measurements in the inlet duct. The results of the analysis are shown in figure 13 for the detailed case of §3.1. The volume source is driven at the observed instability frequency of 65 Hz. Excellent agreement is

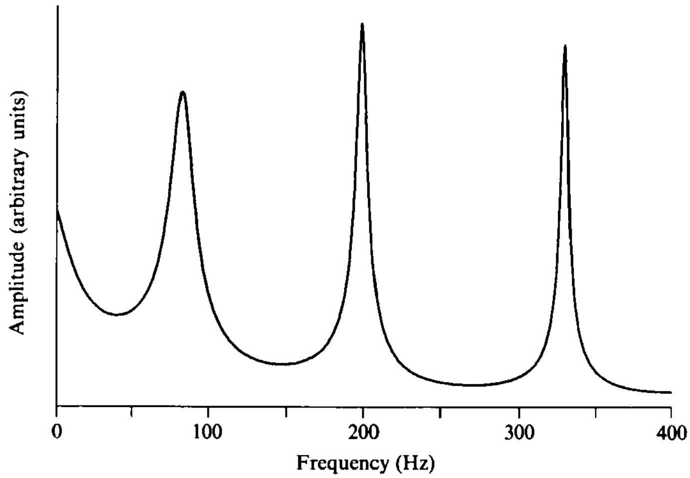

FIGURE 14. Calculation of the acoustic gain *vs.* frequency for the system with the long inlet.

$L = 58$ mm	$L = 80$ mm	$L = 100$ mm	$L = 125$ mm
89	86	83	80
210	204	199	194
342	334	330	325

TABLE 2. Computed values of lower-mode acoustic eigenfrequencies (in Hz) of the system when combustor length L is varied (frequency < 400 Hz)

found between the calculation and the data, indicating that the pressure field is determined by longitudinal mode acoustics.

In the inlet and combustor used here, the acoustic amplification is limited to frequencies within narrow bands around discrete resonant peaks as shown in figure 14. Experimental data, however, show that when the operating conditions are varied, the instability can occur over a wide and continuous range of frequencies. This fact can be attributed to the change in the vortex lifetime which depends on flow speed and combustor length. In comparison, the system acoustic characteristics (table 2) remain relatively unchanged under combustor length modification.

3.2.3. *The short inlet case*

To test equation (1) under a different inlet situation, the inlet length is reduced by more than a half. The two different inlet configurations are compared in figure 15. According to the acoustic analysis of the previous section, the lower longitudinal modes are calculated to be near 184 and 545 Hz for this new configuration. Since the new inlet section is very short and resembles a Helmholtz type resonator, the Helmholtz frequency is also calculated. Assuming the plenum chamber acts as the cavity which provides the stiffness element and the mass of the mixture column in the inlet duct vibrates as a unit, simple Helmholtz resonator theory (Morse & Ingard 1968) gives the fundamental frequency of the system to be 110 Hz.

The general performance of the combustor is not greatly affected by the change; again, flow becomes highly pulsatile at an equivalence ratio of 0.6 and above. In a similar manner as in §3.2.1, a systematic variation of the inlet velocity and combustor length is carried out. Since the acoustic feedback time has been reduced

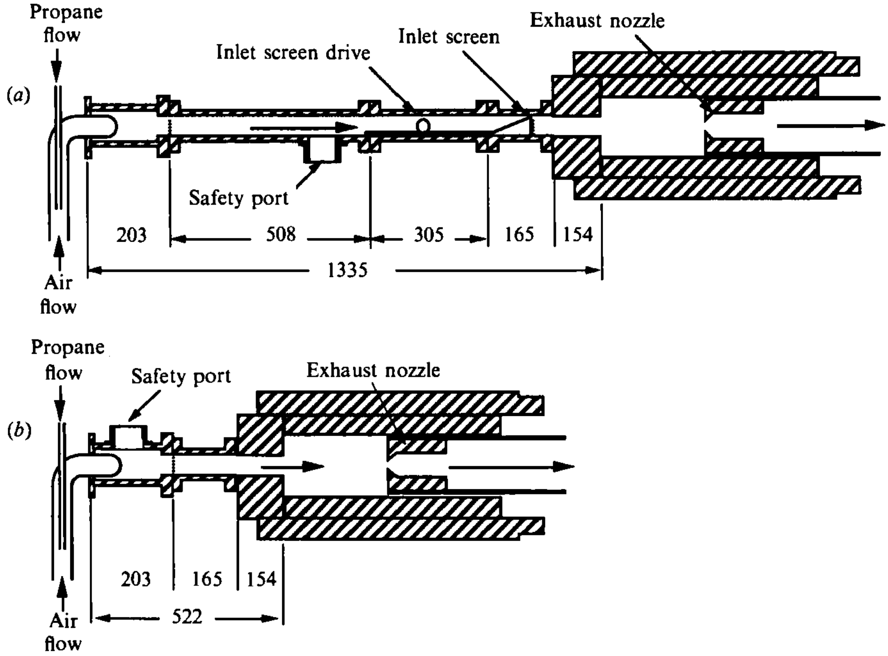

FIGURE 15. New shortened inlet (*b*) shown with the original long inlet (*a*). (Dimension in mm.)

Combustor length (mm)	Inlet velocity (m/s)	Equivalence ratio	Observed instability frequency (Hz)
76	12.3	0.65	85.1
	13.4	0.65	95.3
	14.4	0.65	99.7
	16.5	0.65	112.9
	18.2	0.64	129.0
100	12.3	0.65	79.2
	13.4	0.65	82.1
	14.4	0.65	84.1
	16.5	0.65	88.0
	18.5	0.65	97.8
123	12.3	0.65	68.4
	13.4	0.65	75.3
	14.4	0.65	76.2
	16.5	0.65	82.1

TABLE 3. Instability frequencies observed during various operating conditions (short-inlet configuration)

by shortening the inlet length, equation (1) suggests that the instability will occur at higher frequencies. The results are summarized in table 3. They are consistent with the expectation.

When the instability period is plotted as a function of L/U_{ref} (figure 16), the data fall on a line with a slope of 1.0 and an intercept of 4.5 ms. This time of 4.5 ms is equal to one-half of the Helmholtz period. Since the inlet gas column takes one-half of the fundamental Helmholtz period to reverse the direction of a motion, it is the characteristic response time based on Helmholtz-type feedback. Therefore, given

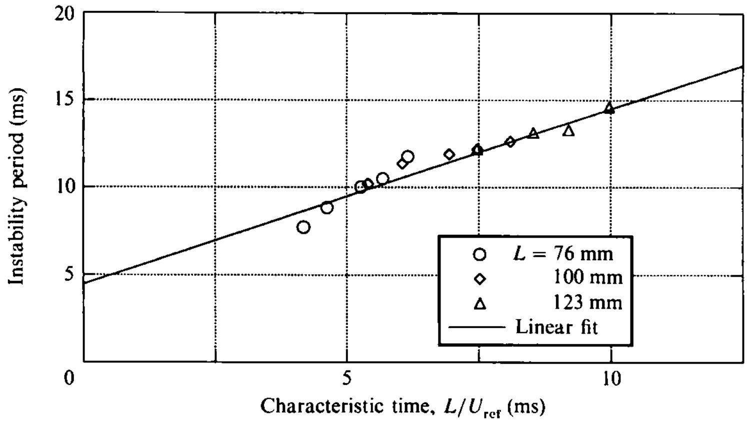

FIGURE 16. Measured period of oscillation as a function of the characteristic flow residence time L/U_{ref} for the short-inlet case.

that the vortex lifetime can be estimated by L/U_{ref}, the instability period is again consistent with equation (1). The observed instabilities under the new configuration can be characterized as mode I type oscillations.

4. Discussion

4.1. *A coupled acoustic–convective instability mechanism*

The results show that the instability frequency is determined by both vortex dynamics in the reaction zone and the acoustic response of the inlet section. The nature of the instability is fundamentally different from classical acoustic modes in which the heat release is driven in phase by and with the acoustic field. The instability mechanism is more similar to that of a series of vented explosions where pressure in the reaction zone is determined by a balance between the energy release rate and the venting rate (Bradley & Mitcheson 1978). This mechanism is based on the modulation of the exhaust mass flux due to alternate flow of burnt and unburnt mixture which drives large pressure variations in the combustor. Appropriately timed heat release from vortex breakdown and burning sustains the cyclic process by pulsing the heat release in phase with the pressure variations.

Now consider a positive perturbation in the amount of reactants delivered to the combustor. A positive perturbation in velocity at the dump plane results in additional vorticity being injected into the combustor. When the perturbation is large enough, the flame sheets move and roll-up into a vortical structure. As the structure is convected through the combustor, it grows in size, increasing the flame-front surface area, and the reaction rate increases. The pressure rises as long as the heat release rate is large in comparison to the venting rate. As the pressure rises, the inlet responds by reducing the flow velocity, thus limiting the amount of reactants being admitted. In addition, once the vortex reaches the nozzle, the composition of the exhaust material is abruptly changed and the exit mass flow rate increases significantly. Consequently, the balance between venting and heat release changes sign and the pressure drops in the combustion chamber. After a certain delay time which characterizes the inlet response to the combustor pressure variation, a new perturbation of the inflow rate is triggered at the combustor inlet. The amplitude and phase of this perturbation is determined by the nature and geometry of the inlet and its response to pressure variations in the combustor. For a long and narrow inlet pipe, acoustic wave propagation will determine the inlet response. In the case of a short inlet with a plenum chamber, Helmholtz-resonator-type dynamics control the admission of fresh reactants.

In mode I type oscillations, the timing between a vortex burning and the next shedding is determined by the acoustic response of the inlet. If this response time is sufficiently long compared to the vortex lifetime, then it seems plausible that there could be more perturbations before the characteristic response time completely elapses. During this time lapse, should some of the perturbations be strong enough to shed a large vortical structure and independently start their own chain mechanism, then the apparent instability frequency will be increased from the mode I frequency by an integral factor representing the number of superposed loops. This explains the occurrence of higher-mode oscillations.

It may be worth noting that, in this mechanism, the vortex shedding at the limit cycle is driven by inlet acoustics and is not associated with hydrodynamic instability modes. For all the unstable regimes we have studied, a single large vortex structure is generated at each cycle and dominates any smaller scale vorticity which might be produced in the jet shear layers (Trouvé, Candel & Daily 1988).

4.2. *Instability mode selection*

Equation (1) represents the global feedback loop required for a self-sustained type oscillation. It is a simple expression of a phase criterion which merely closes the loop in a resonant manner. The feedback loop is formed by downstream-convected vortical structures which produce strong velocity perturbations when they impinge and burn and the inlet acoustics which respond and convert the perturbations back to positive. The equation combines acoustic and convective features of the system in a very simple way, and shows the dual nature of the instability mode. Also it is consistent with the experimental observations of §3.2.

Somewhat similar arguments, based on matching conditions for characteristic times, have been used to explain hydrodynamic instabilities in non-reacting flows (Ho & Nosseir 1981; Martin, Brooks & Hoad 1985; Jou & Menon 1986). In the current mechanism, however, the inlet participates actively in organizing the vortices, making it necessary to know the acoustic characteristics of the inlet. Also, owing to the presence of the reacting flow, the heat release process dominates over any hydrodynamic or acoustic amplification and becomes an important selection mechanism among an infinite number of possible modes which satisfy the global feedback loop equation.

As discussed in §3.1.3, to sustain a large-amplitude oscillation, Rayleigh's criterion needs to be satisfied. A simplified expression of Rayleigh's criterion can be obtained independently of equation (1) by using linear acoustic theory combined with experimental observations. According to linear acoustic theory, we assume that the acoustic velocity and pressure at the combustor inlet vary sinusoidally in time with velocity leading pressure by 90°. Also, based on our experimental observations, we assume that vortices are shed at the instant of maximum acceleration as shown in figure 17. If we further assume that the burning of the vortices occur after τ_v, then a positive feedback in the Rayleigh sense requires τ_v to be in the following range:

$$\tfrac{1}{4}T_i < \tau_v < \tfrac{3}{4}T_i \qquad (2)$$

Now combining (1) and (2), the following condition for sustaining an oscillation at mode N is obtained:

$$\frac{1}{4N-1} < \frac{\tau_v}{\tau_f} < \frac{3}{4N-3}. \qquad (3)$$

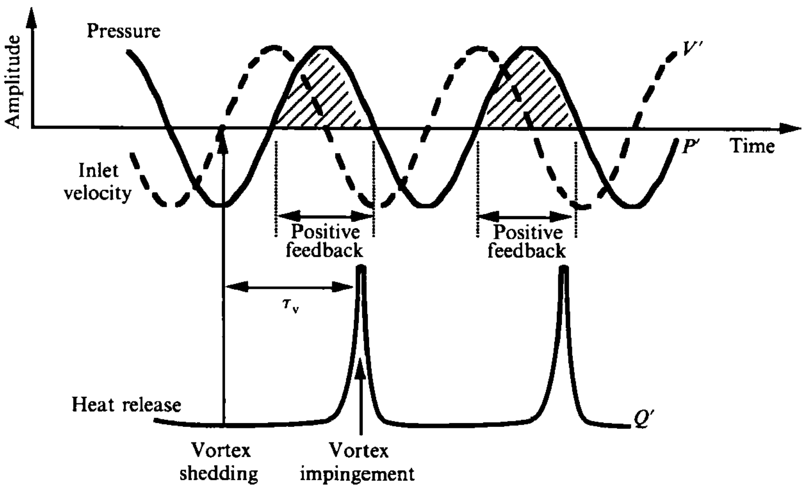

FIGURE 17. An illustration of Rayleigh's criterion for pulsating combustion modes.

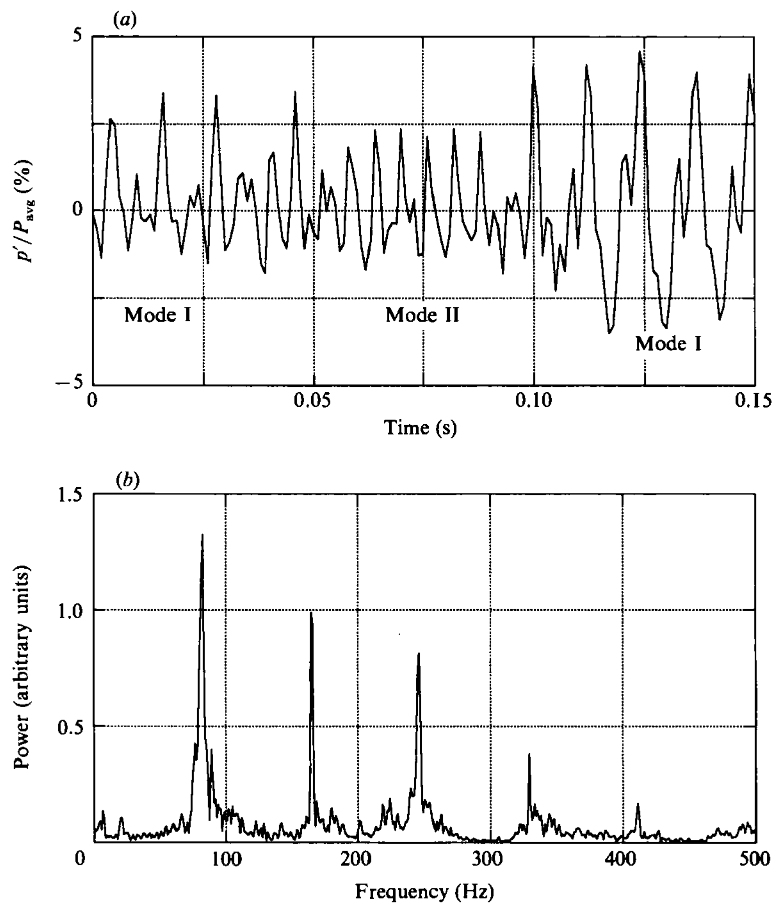

FIGURE 18. Intermittent mode switching behaviour observed at some operating conditions. (*a*) Pressure records, (*b*) corresponding power spectrum.

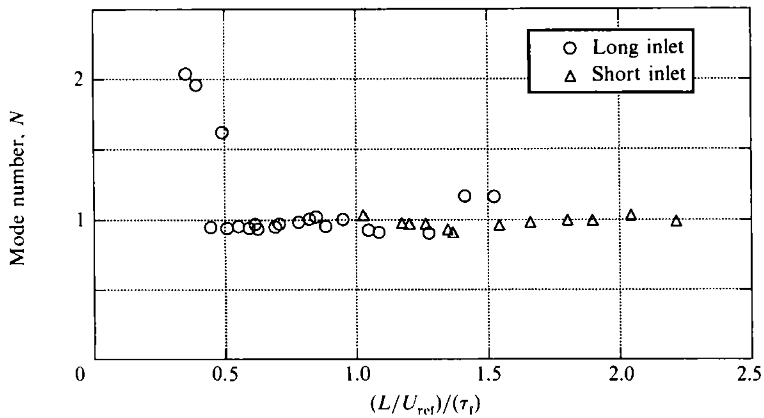

FIGURE 19. Mode number N as a function of the ratio L/U_{ref} over τ_f.

This constraint may be used to determine the range of occurrence of each mode. For example, mode I oscillation ($N = 1$) requires the ratio between τ_v and τ_f to be in the range from $\frac{1}{3}$ to 3 and mode II from $\frac{1}{7}$ to $\frac{3}{5}$. There exists a region of overlap between the two modes, which may correspond to a possible transition from one oscillatory regime to the other. Some of the data taken at the overlap region show this behaviour. Figure 18(a) shows a combustor pressure record when the ratio is 0.4. In these conditions, the oscillation appears to switch intermittently between the two modes. The corresponding long-time-averaged power spectrum shows peaks at both frequencies associated with each mode (figure 18b). When the mode number N is plotted (figure 19) for the experimental data of §3.2, very good agreement is found with (3). In particular, it shows clearly why only the first-mode oscillations or only a combination of first- and second-mode oscillations could be observed in the range of operating conditions tested.

One note of a practical concern is how to estimate the vortex lifetime. In low-frequency instabilities, this characteristic time is essentially a convection time since the chemical reaction time tends to be negligible in comparison. An earlier study (Smith 1985) has shown that the propagation of vortices is primarily governed by the magnitude of pressure and velocity fluctuations – a quantity that depends on the operating conditions and thus very difficult to predict. In the present study, however, the convection time is shown to scale mainly with the combustor length L and a mean convection speed U_{ref}. Although the choice of U_{ref} in an unsteady environment may seem somewhat arbitrary, the following observations support the importance of the mean inlet flow velocity in determining the vortex lifetime: first, the shedding of vortices appears to be synchronized with the instant of maximum acceleration which occurs when the velocity is at its mean value; and second, since the amplitude growth saturation during instability initiation appears to be limited by flow reversal, the amplitude of mean velocity also gives the magnitude of velocity fluctuations at the limit cycle.

The data are now re-plotted (figure 20) together with the predictions from (1) and (3). Some deviations are believed to be due to errors in estimating the vortex lifetime by L/U_{ref}. For example, one regime when the combustor length is 80 mm exhibits pressure oscillations at much lower amplitude (less than 5% of the mean) in comparison with other cases. Then it seems likely that the vortex convection speed is lower than U_{ref} and consequently L/U_{ref} is an underestimate of the vortex lifetime. Also, in the case of a 150 mm long combustor, since a typical reattachment length of

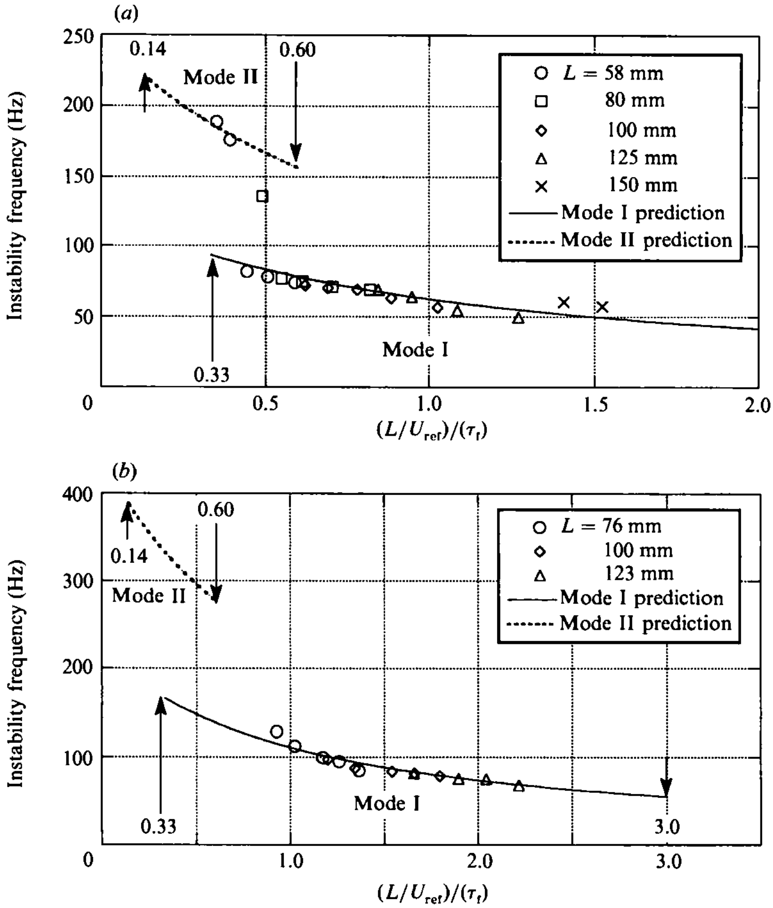

FIGURE 20. Instability frequency predictions and comparison with the experimental data. (*a*) Long-inlet configuration. The inlet response time $\tau_f = 8.0$ ms. (*b*) Short-inlet configuration. The inlet response time $\tau_f = 4.5$ ms.

the reacting flow (5 to 7 step heights for an isothermal flow according to Eaton & Johnston 1980; and 30% less for a reacting flow according to Pitz & Daily 1983) is shorter than the combustor length, the destruction of vortices may occur before they reach the exhaust nozzle. In that case, L/U_{ref} gives an overestimate of the vortex lifetime.

However, in spite of the discrepancies, overall agreement between the experimentally observed frequencies and the predictions of mode I and mode II oscillations are remarkably good. Also, the observed transition from one mode to another is very well predicted. When the predictions indicate more than one possible mode, it probably implies that mode hopping and hysteresis effects are to be expected. Under these conditions, the experiments show that oscillations switch intermittently from one mode to another.

5. Summary and conclusion

This paper describes a low-frequency vortex-driven pulsating combustion mode in a dump cavity which features an abrupt contraction at the outlet. The instability is particularly intense and exhibits periodic vortex shedding, flow reversal, flashback in the inlet duct, and partial extinction in the combustor. The inlet-duct acoustics sustain large velocity fluctuations and induce vortex shedding at the combustor dump plane when flow acceleration is maximum. The vortices then convect and impinge on the exhaust nozzle, causing a break-up into small-scale structures and completing the mixing of cold fresh reactants and hot burnt products. Maximum heat release from combustion follows shortly with appropriate phase difference which satisfies Rayleigh's criterion.

The inlet acoustic field is well predicted by a linear one-dimensional calculation. For the case of compact combustion, the global features of the acoustic field are quite insensitive to the details of the combustion process. A harmonic Dirac source representation allows good agreement between the experimental and the computed pressure fields. However, while the acoustic gain of the system is concentrated around discrete peaks, the combustion system exhibits a piecewise continuous spectrum of unstable modes. The ability of the combustion system to sustain oscillations over a wide range of frequencies demonstrates that the acoustic description is insufficient. It also underlies the importance of vortex dynamics in controlling the instability mechanism and in determining the instability frequency.

Systematic analysis of the flow features inside the combustion chamber shows that the resonant period of oscillation is determined by the sum of the vortex convection time in the combustor and the acoustic feedback time in the inlet. This behaviour is quite unusual and differs from classical acoustic models. It is believed to be an essential feature of combustors with an exit nozzle. In this kind of configuration, vortex impingement on the nozzle drives a strong modulation of the exhaust mass flux and forces large pressure variations inside the combustor. This process is similar to that occurring in a vented explosion where pressure in the reaction zone rises and falls according to a balance between the energy release rate and the venting rate. Also such processes are repeated in a cyclic manner as the inlet acoustics provide a convenient timing mechanism between the succession of events. It is then suggested that the combustion instability should be viewed as a coupled acoustic–convective mode.

Experimental observations using the phase-sensitive schlieren imaging technique show that the vortical structures are shed when acceleration is at a maximum. A good approximation of the vortex lifetime, which includes convection through the combustor, impingement on the exhaust nozzle, breakdown into small-scale structures and burning, is also provided by the ratio of the combustion chamber length L over the inlet mean velocity U_{ref}. Our data suggest that this result may be applicable to all cases in which the exhaust nozzle interferes with a vortex trajectory and determines its lifetime.

Based on these observations, a reasonable prediction of the instability frequencies is possible. One important parameter in determining the frequencies appears to be the ratio of τ_{v} to τ_{f}. The general prediction procedure may be summarized as follows:

Step 1: Using acoustic theory, estimate τ_{f}, which is the inlet section response time to pressure variations in the combustor. This characteristic time is that between maximum pressure in the combustor and maximum acceleration at the inlet. For low-Mach-number flows with constant speed of sound, this reduces to a function of geometry only.

Step 2: Estimate τ_{v}, which is the characteristic time associated with vortex history. For short combustors with low Mach numbers, L/U_{ref} provides a good approximation.

Step 3: Using the global feedback loop equation (1) and Rayleigh's criterion (2), determine which mode(s) can occur. Mode hopping and hysteresis effects are to be expected when more than one mode is predicted.

The research described in this paper has been supported by Office of Naval Research Grant N00014-84-K-0372. The experimental work was conducted at the University of California at Berkeley. Some analysis was conducted at the University of Colorado at Boulder, and Ecole Centrale de Paris. The authors would like to acknowledge the many helpful conversations with numerous colleagues, most especially S. Candel, T. Poinsot and F. Culick, and graduate students L. Bauwens, R. Keanini and A. Ghafourian.

REFERENCES

ABOUSEIF, G. E., KEKLAK, J. A. & TOONG, T. Y. 1984 Ramjet rumble: the low frequency instability mechanism in coaxial dump combustors. *Combust. Sci. Tech.* **36**, 83–108.

BRADLEY, D. & MITCHESON, A. 1978 The venting of gaseous explosions in spherical vessels. I-theory. *Combust. Flame* **32**, 221–236.

CHU, B. T. 1956 On the energy transfer to small disturbances in a viscous compressible heat conductive medium. *AFOSR Contractor Rep.*, Johns Hopkins University.

CRUMP, J. E., SCHADOW, K. C., YANG, V. & CULICK, F. E. C. 1986 Longitudinal combustion instabilities in ramjet engines: identification of acoustic modes. *J. Propulsion Power* **2**, 105–109.

EATON, J. K. & JOHNSTON, J. P 1980 Turbulent flow reattachment: an experimental study of the flow and structure behind a backward-facing step. *Rep.* MD-39. Stanford University.

HEGDE, U. G., REUTER, D., ZINN, B. T. & DANIEL, B. R. 1987 Fluid mechanically coupled combustion instabilities in ramjet combustors. *25th Aerospace Sciences Meeting, Reno, NV, Paper* 0216.

HO, C. M. & NOSSEIR, N. S. 1981 Dynamics of an impinging jet. Part 1. the feedback phenomenon. *J. Fluid Mech.* **105**, 119–142.

HUMPHREY, J. W. & CULICK, F. E. C. 1987 Linear and nonlinear stability of acoustics with nonuniform entropy in chambers with mean flow. *19th Fluid Dynamics, Plasma Dynamics and Lasers Conf., Honolulu, HW, Paper* 1417.

JOU, W. H. & MENON, S. 1986 Numerical simulation of the vortex-acoustic wave interaction in a dump combustor. *24th Aerospace Sciences Meeting, Reno, NV, Paper* 0002.

JOU, W. H. & MENON, S. 1987 Simulations of ramjet combustor flow fields. Part II. origin of pressure oscillations. *19th Fluid Dynamics, Plasma Dynamics and Lasers Conf. Honolulu, HW, Paper* 1422.

LANGHORNE, P. J. 1988 Reheat buzz: an acoustically coupled combustion instability. Part 1. experiment. *J. Fluid Mech.* **193**, 417–443.

MARBLE, F. E. & CANDEL, S. M. 1977 Acoustic disturbance from gas non-uniformities convected through a nozzle. *J. Sound Vib.* **55**, 225–243.

MARTIN, R. M., BROOKS, T. F. & HOAD, T. R. 1985 Reduction of background noise induced by wind tunnel jet exit vanes. *AIAA J.* **23**, 1631–1632.

MORSE, P. M. & INGARD, K. U. 1968 *Theoretical Acoustics.* McGraw-Hill.

PITZ, R. W. & DAILY, J. W. 1983 Combustion in a turbulent mixing layer formed at a rearward-facing step. *AIAA J.* **21**, 1565–1570.

POINSOT, T., TROUVÉ, A., VEYNANTE, D., CANDEL, S. M. & ESPOSITO, E. 1987 Vortex driven acoustically coupled combustion instability. *J. Fluid Mech.* **177**, 265–292.

PUTNAM, A. A. 1971 *Combustion Driven Oscillations in Industry.* Elsevier.

RAYLEIGH LORD 1878 The explanation of certain acoustic phenomena. *R. Inst. Proc.* **8**, 536–542.

RAYLEIGH LORD 1945 *The Theory of Sound*, p. 227. Dover.

ROCKWELL, D. 1983 Oscillations of impinging shear layers. *AIAA J.* **21**, 645–664.

ROGERS, D. E. & MARBLE, F. E. 1956 A mechanism for high frequency oscillations in ramjet combustors and afterburners. *Jet Propulsion* **26**, 456–462.

SCHLICHTING, H. 1979 *Boundary Layer Theory*, pp. 436–438. McGraw Hill.

SMITH, D. A. 1985 An experimental study of acoustically excited, vortex driven, combustion instability within a rearward facing step combustor. PhD thesis, California Institute of Technology.

SMITH, D. A. & ZUKOSKI, E. E. 1985 Combustion instability sustained by unsteady vortex combustion. *21st Joint Propulsion Conf., Monterey, CA, Paper* 1248.

STERLING, J. D. & ZUKOSKI, E. E. 1987 Longitudinal mode combustion instabilities in a dump combustor. *25th Aerospace Sciences Meeting, Reno, NV, Paper* 0220.

TROUVÉ, A., CANDEL, S. M. & DAILY, J. W. 1988 Linear stability of the inlet jet in a ramjet dump combustor. *26th Aerospace Sciences Meeting, Reno, NV, Paper* 0149.

TROUVÉ, A., YU, K. & DAILY, J. W. 1987 Phase sensitive schlieren system for studying periodic combustion phenomena. *Joint Meeting of the Western States Section of the Combustion Institute, Honolulu, HW.*